Low Temperature Rapid Curing of Polymer Dielectrics on Metallized Organic Laminates by Variable Frequency Microwave Processing

Taehyun Sung, Sue A. Bidstrup Allen and Paul A. Kohl*
School of Chemical and Biomolecular Engineering
Georgia Institute of Technology
Atlanta, GA 30332-0100, USA
Ph: 404-894-2893; Fax: 404-894-2866
Email: paul.kohl@chbe.gatech.edu
*-Corresponding author

Abstract

The curing of polymer dielectrics on organic laminates by variable frequency microwave (VFM) processing was studied. Polymer dielectrics, such as polyimides, normally require long cure times at elevated temperatures resulting in processing incompatibility with epoxy-based laminates due to the low thermal stability of the organic laminates. In this study, VFM processing was investigated as an alternative, low temperature technique for curing polyimide and benzycyclobutene (BCB) on metallized bismaleimide triazine/epoxy (BT) board. The VFM heating characteristics of the metallized (BT) boards were studied. The VFM heating rates of the BT boards strongly depended on the configuration, size, and shape of the copper patterns on the boards. The VFM curing of polyimide and BCB on the metallized BT boards was also performed. The curing condition was optimized to minimize board degradation. At the same board degradation level, the chemical, thermo-mechanical and electrical properties of the VFM cured film were compared with a film thermally cured using a conventional convection furnace. A higher degree of curing and lower dielectric constant was achieved for benzocyclobutene (BCB) films on BT boards processed using VFM curing than was obtained using conventional curing. VFM cured polyimide (PI 2611) showed a similar degree of curing and Young's modulus to conventionally cured PI 2611. However, the VFM cured PI 2611 showed a higher residual content solvent and a higher dielectric constant than conventionally cured PI 2611.

Key words

Benzocyclobutene, microwave heating, organic laminates, polyimide.

1.0 Introduction

The increasing demand for high speed and high performance electronic devices has driven the substrate and board design toward smaller feature sizes and higher levels of integration [1]. To fully utilize high-speed silicon devices and to accommodate an increasing number of I/Os, higher density substrates are required [2], [3]. For cost effective, high density substrates with rapid and uniform signal propagation, it is desirable to replace epoxy-based dielectrics with lower dielectric constant polymers, such as polyimide and benzocyclobutene (BCB), for dielectric build-up layers on metallized organic laminates [2].

However, the curing of low-k polymer dielectrics on organic laminates is limited by the low thermal stability of the traditional laminate systems. Commercially available organic substrates have a low glass transition temperature. For example, the glass transition temperature for a fiberglass reinforced epoxy (FR-4) substrate ranges between 140 and 160°C, and for a bismaleimide triazine/epoxy (BT) substrate is approximately 185°C [6]. Typically, polyimide dielectrics are cured at 350°C for 1hr [4]. The curing temperature of BCB dielectrics ranges from 220°C to 250°C depending on cure time [5]. Processing above the glass transition temperature of the organic

substrate for extended time periods can cause either the delamination or the degradation of the laminated substrate.

In this study, variable frequency microwave (VFM) processing was investigated as an alternate curing technique to curing in a conventional convection furnace. VFM processing produces a more homogeneous electric field distribution than single frequency microwave system through the use of rapid frequency sweeping [7]. VFM processing has been reported to be an effective rapid curing technique for polyimides [8, 9] and BCB [10]. In addition, the feasibility of VFM curing of polyimides on FR-4 board was previously studied by Tanikella [11]. However, the detailed interaction of microwaves with patterned metal on organic laminates and its effect on the board degradation and the polymer curing have not been reported. The first objective of this study was to investigate the VFM heating characteristics of the organic laminates with copper metallization. The second objective was to study the VFM curing of polyimide and BCB on the metallized BT boards.

2.0 Microwave Heating

The principal mechanism of microwave heating of polymeric materials is through dipole polarization by the electric field. The average power per unit volume converted into heat (P_{ave}) by a material is given by the following equation [12].

$$P_{ave} = \pi f \varepsilon_0 \varepsilon' \tan\delta E_{rms}^2, \quad (1)$$

where E_{rms} is the root mean square electric field strength, ε_0 is the permittivity of free space, ε' is the dielectric constant, $tan\delta$ is the loss tangent, and f is the frequency.

Electrons move freely in metals under an alternating electric field. However, the electronic conduction is confined within a very thin surface layer or 'skin'. At a metal thickness greater than the skin depth, the metal becomes reflective to microwaves and is not easily heated [12]. The skin depth, δ_s, is defined as the depth into the conductor at which the current density is 1/e of its value at the surface. It is related to the properties of the materials in the following equation,

$$\delta_s = \sqrt{\frac{2}{\sigma \omega \mu}}, \quad (2)$$

where σ is conductivity, μ is permeability and ω ($2\pi f$) is the angular frequency.

3.0 Experimental

The polymers studied in this work were Hitachi-Dupont Microsystems (Wilmington, DE) PI 2611 and Dow Chemical Company (Midland, MI) Cyclotene 3022. PI 2611 is a non-photosensitive polyimide. The backbone of PI 2611 is based on 3,3'-4,4'-biphenyltetraccarboxylic acid and P-phenylenediamine (BPDA/PPD). The solvent in PI 2611 is N-methyl-2-pyrollidone (NMP), and its boiling point is 202°C. The standard curing condition of PI 2611 recommended by the manufacturer involves heating at 350°C for 1hr. Cyclotene 3022 is a thermoset resin based on the benzocyclobutene (BCB) monomer. The resin is received as B-staged and dissolved in mesitylene. The boiling point of mesitylene is 165°C. The standard curing condition of Cyclotene 3022 recommended by manufacturer is to process at 250°C for 1hr.

A double copper clad BT board (G 200) manufactured by Isola Laminated Systems Corp. (La Crosse, WI) was used as an organic laminate. The glass transition temperature of G 200 is 185°C [6]. The thickness of the copper cladding was approximately 20 μm, as measured by an Alphastep-500 profilometer.

The VFM system used in this study was a Microcure 2100™ furnace manufactured by Lambda Technologies Inc. (Morrisville, NC). The Microcure 2100 ™ unit has five control parameters: the central frequency, the frequency bandwidth, the sweep rate, the power output and the ramp rate. The central frequency can be tuned from 5.85 to 7.0 GHz. Frequency bandwidth varies from 0 to 10%. The sweep time ranges from 0.1 to 60 seconds. The maximum power output is 500 W. The ramp rate is adjustable from 0.1 to 10°C/sec. The samples were processed at either a constant power or a constant ramp rate in a nitrogen environment. At a constant ramp rate, the power is automatically controlled to achieve the desired ramp rate. A central frequency of 6.425 GHz, 0.15 GHz bandwidth, and 0.1 second sweep time were used through out this study. Unless specified, all the samples were processed on a quartz substrate in a nitrogen environment. The PI 2611 and Cyclotene 3022 samples were soft-baked at 120°C for 2 min before regular curing process.

The temperatures were measured using a Nortech fiber optic probe or a Raytek Thermalert T30 series pyrometer. The Nortech fiber optic probe is a contact probe and is thermally stable up to 210°C. For higher temperature measurements, a non-contacting Raytek Thermalert T30 series pyrometer was used. The pyrometer was calibrated for the emissivity of each sample.

The curing reaction was monitored by using Fourier transform infrared spectroscopy (FT-IR). FT-IR spectra were collected in the attenuated total reflection (ATR) mode using a Nicolet Magna-IR Fourier transform infrared spectrometer. All spectra were recorded at a resolution of 4 cm^{-1} and averaged over 128 scans. The curing reaction of PI 2611 is the ring closure reaction between amide group and carboxylic acid in the backbone and forms an imide ring as shown in Fig. 1. The peak at 1370 cm^{-1}, corresponding to C-N-C stretching of the imide ring, was used to monitor the formation of the imide ring. The peak at 1516 cm^{-1}, corresponding to ring breathing vibration of 1, 4 substituted benzene, does not change during the curing and was used as an internal reference. The degree of curing of PI 2611 was calculated according to (3).

$$\text{Degree of cure (\%)} = \frac{(A_{1370\ cm^{-1}} / A_{1516\ cm^{-1}})_{sample}}{(A_{1370\ cm^{-1}} / A_{1516\ cm^{-1}})_{full\ cure}} \times 100 \quad (3)$$

where A_{1370cm}-1 and A_{1516cm}-1 are the absorbance of the 1370cm^{-1} and 1516 cm^{-1} peaks, respectively. The absorbance of fully cured PI 2611 was determined from a film for which 100% degree of curing is assumed. 100% degree of curing was achieved by curing at 350°C in a standard convection furnace for 1 hour.

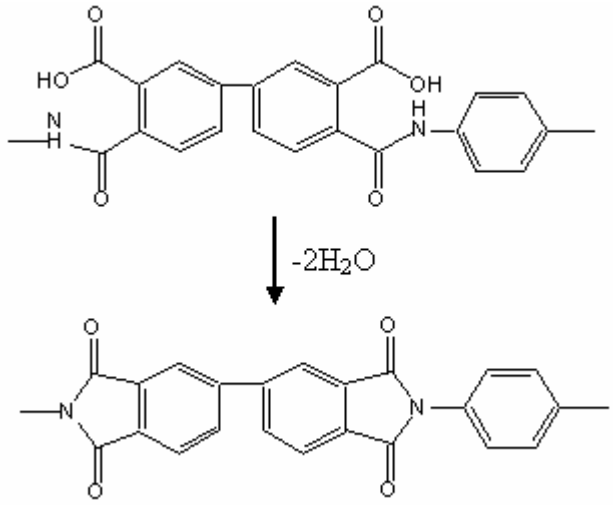

Fig. 1. The structure and curing reaction of PI 2611.

The curing reaction of Cyclotene 3022 is a two-step reaction as shown in Fig. 2. The first step in the curing is the opening of a four-member ring of BCB to produce an o-quinodimethane intermediate. The second step is the Diels-Alder reaction between the o-quinodimethane intermediate and the alkene groups in the prepolymer to form a tri-substituted tetrahydronaphthalene. The peak at 1500 cm^{-1}, corresponding to a vibration of the tetrahydronaphtlalene, was used to monitor the curing reaction. The peak at 1253 cm^{-1}, corresponding to the rocking mode of the methyl groups attached to the silicon atoms, was used as an internal reference. The degree of curing of Cyclotene 3022 was also calculated according to (3), replacing the absorbance of the 1370 cm^{-1} peak with the absorbance of the 1500 cm^{-1} peak and replacing the absorbance of the 1516 cm^{-1} peak with the absorbance of the 1253 cm^{-1} peak. Fully cured Cyclotene 3022 was achieved by curing at 300°C for 1hr [10]. The standard curing condition of Cyclotene 3022 recommended by the manufacturer (i.e. curing at 250°C for 1hr) resulted in 95% degree of curing [5].

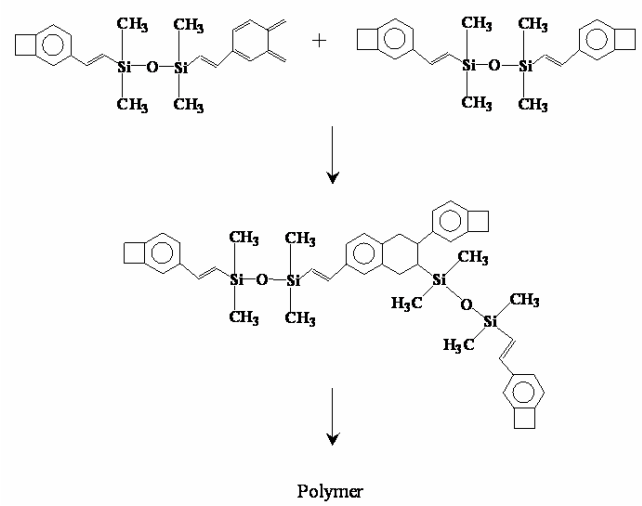

Fig. 2. The structure and curing reaction of Cyclotene 3022

The Young's modulus, the thermal stability, and the electrical properties were obtained for the polymer film cured on the full surface copper clad BT board. The 500 Å thick titanium layer was deposited by DC sputter on top of the copper clad BT board prior to polymer deposit. A titanium layer was used as a sacrificial layer to facilitate the lift-off of the polymer film from the substrate. It was shown in a separate experiment that the VFM heating rate did not change by depositing the 500Å thick titanium layer [13].

The Young's modulus of the polymer film was calculated from the stress versus strain curves obtained from a tensile test of free-standing films using an Instron tensile tester (Model 5640). Rectangular strips of the polymer film of size 45mm in length and 9mm wide films were prepared for tensile testing. Films were cut into desired dimension before lifting off the substrate and then dried in the vacuum oven for 12 hours after the lift-off process to remove the moisture. The tensile test was performed in 5 mm/min

extension rate at room temperature.
The thermal stability of PI 2611 and Cyclotene 3022 was determined by thermo-gravimetric analysis (TGA) using a Seiko TG / DTA analyzer. Five to ten mg of a polymer film were placed in a TGA pan and ramped at 10ºC/min to 450°C. The weight loss during the temperature ramp was recorded, and the thermal stability was reported as a 1% weight loss temperature.

The dielectric constant and the loss tangent were measured using a parallel plate capacitor structure. The polymer films were cured on the full surface copper clad BT boards, and a top plate was fabricated from sputtered titanium (200Å) and aluminum (1000Å) layers. The capacitance and the conductance were measured using a HP4236 LCR meter at 10 kHz on a Karl Suss Probe station. The dielectric constant (ε') and loss tangent ($tan\delta$) were determined from the capacitance, C, and conductance, G, using (4) and (5):

$$C = \frac{\varepsilon_0 \, \varepsilon' \, A}{t} \tag{4}$$

$$G = \omega C \tan\delta \tag{5}$$

where ε_0 is the permittivity of vacuum (8.85×10^{-12} F/m), A is the area of the top electrode, t is the thickness of the film, $\omega = 2\pi f$, where f is the measurement frequency and is the loss tangent. The measurements were performed at the frequency of 10 kHz.

The double copper clad BT boards were etched to form a variety of copper patterns using photolithography and wet etching. After the copper patterning, the BT board was rinsed in distilled water and dried in the vacuum over for 12 hours. Pattern shapes includes squares, circles, and lines.

The degradation level of the BT board after the VFM curing was determined by comparing its appearance to the appearance of control samples. The BT boards were thermally degraded in a nitrogen filled furnace at different conditions and used as controls. Degradation conditions chosen in study were 200°C for 1hr, 220°C for 1hr, 220°C for 3hr, 240°C for 1hr, and 240°C for 3hr. The color of the BT board becomes darker as it degrades. The VFM processed BT boards were visually compared to the control BT boards and reported as equivalent color changes. For example, a board degradation level of '200°C, 1hr' means that the color of the BT board is the same as the BT board thermally degraded at 200°C for 1hr in the nitrogen environment. According to the manufacturer, the board degradation level, 220°C for 1hr, is the maximum acceptable board degradation level in industry. The VFM curing conditions were optimized not to exceed the board degradation level of 220°C for 1hr.

4.0 Results

The VFM heating characteristics of full surface copper clad BT boards were investigated to study the effect of the 20 μm thick copper cladding. The full surface copper clad BT boards have four possible configurations: a double copper clad BT board (i.e., copper on both the top and bottom surface), a BT board with a copper cladding on top surface, a BT board with a copper cladding on the bottom surface, and the bare BT board without copper. The heating characteristics of copper clad BT boards cured on a quartz substrate and suspended in the VFM were investigated.

The VFM heating curves of BT boards without the quartz substrates (i.e. suspended samples) are shown in Fig. 3. The heating rate of the double copper clad BT board is similar to that of the bare BT board. The heating rate of the BT board with a copper cladding on the top is similar to that of the BT board with a copper cladding on the bottom. However, the heating rate of the BT board with a copper cladding on the top or the bottom is significantly lower than those of the bare BT board and the double copper clad BT board.

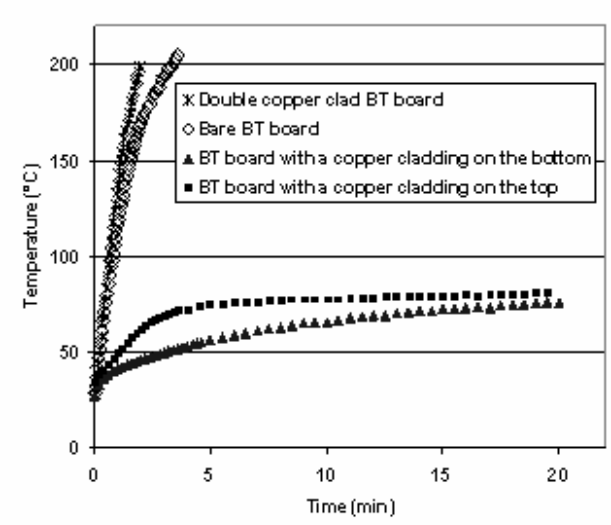

Fig. 3. The VFM heating curves of the full surface copper clad BT boards without the quartz substrate at the constant microwave power of 500 W.

Fig. 4 shows the heating curves of the full surface copper clad BT boards cured on the quartz substrate in the VFM. The heating characteristics differ significantly from those observed in Fig. 3. The heating rate of the BT board with a copper cladding on the top is much higher when placed on

the quartz substrate compared to the heating rate without the quartz substrate. The heating rate of the bare BT board decreases significantly on the quartz substrate, as compared to without the quartz substrate. The heating rate of the bare BT board is lower than that of the BT board with a copper cladding on the top when they are cured on the quartz substrate. The heating rate of the double copper clad BT board and the BT board with a copper cladding on the bottom does not change when placed on the quartz substrate compared to without the quartz substrate. Therefore, it is evident that the quartz substrate does not act simply as a heat sink.

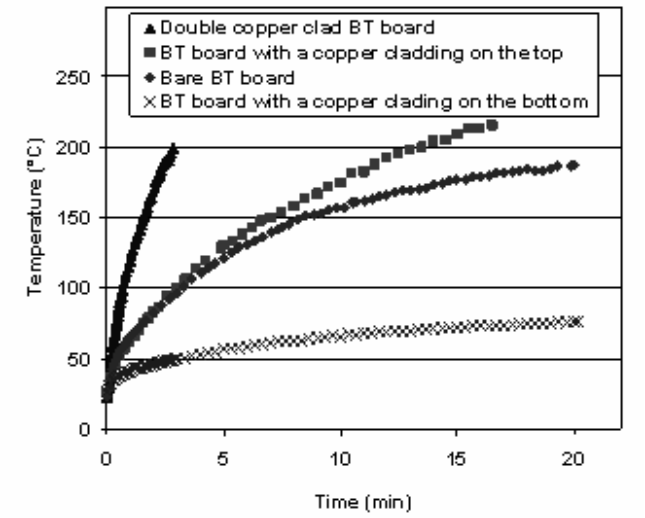

Figure 4. The VFM heating rates of the full surface copper clad BT boards on a quartz substrate at the constant microwave power of 500 W.

The effect of the board edge on the heating rate was examined by covering the edge of a double copper clad BT board with copper tape. As shown in Fig. 5, when the edge opening was covered with copper tape, the heating rate was significantly less than when the edges were open. This effect was observed both with and without the quartz substrate. Hence, it was demonstrated that microwave transmission within the board (between the two copper layers) is minimized when the edges of the board are covered with copper tape.

The effect of patterned copper features on the heating rate of the board was also investigated. Fig. 6 shows the VFM heating curves of BT boards with 100 μm wide lines extending across the entire board and with BT boards that contain broken lines (each segment of the broken line being 100 μm in width × 9 mm in length) at the microwave power of 200 W. The BT board with the broken lines heats much faster than the BT board with the straight lines when there is no full surface copper cladding on the bottom. When there is a full bottom surface of copper cladding, the heating rate

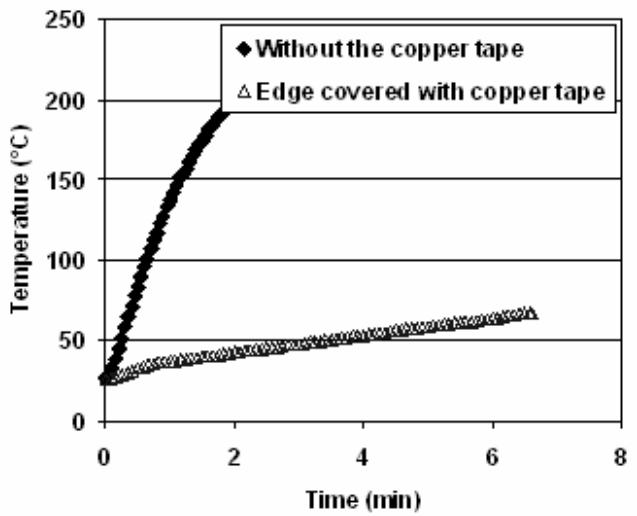

Fig. 5. The heating curves of the double copper clad BT and the double copper clad BT board where the edge opening is covered.

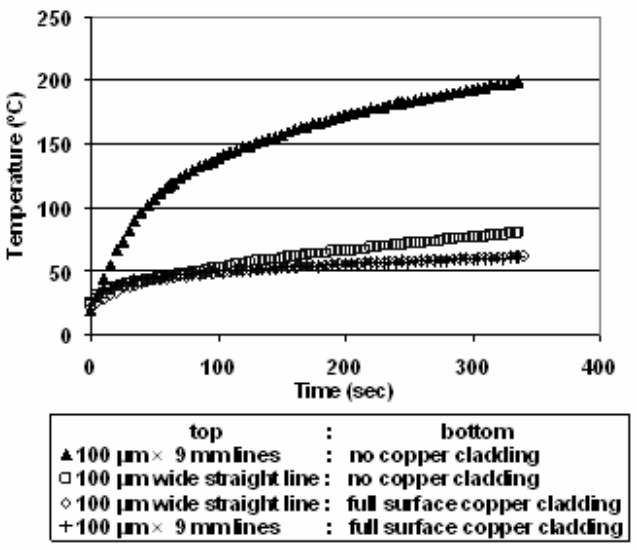

Fig. 6. The VFM heating curves of BT boards with 100 μm wide copper lines at a constant microwave power of 200W.

of the BT board with broken lines is similar to that of the BT board with the straight lines. However, as shown in Fig. 7, at a higher microwave power 300W, the BT board with the broken lines heats faster than the BT board with straight lines.

Fig. 8 shows the effect of copper pattern size on the VFM heating rates of the square copper on top of the BT boards.

The bottom of the board is covered with a full surface of copper cladding. The heating rate of the sample without the quartz substrate increases as the area ratio (i.e. ratio of the

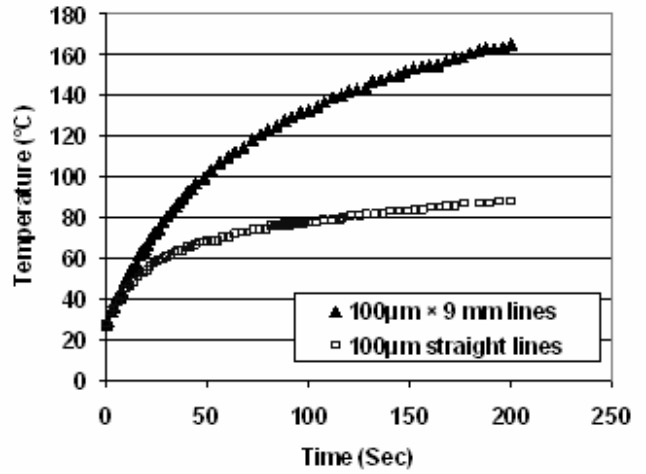

Fig. 7. The VFM heating curves of the BT board with 100 µm wide copper lines on top and the full copper cladding on the bottom at a constant microwave power of 300 W.

area of the square copper pattern to area of the copper cladding on the bottom surface of the board) decreases. On the quartz substrate, the heating rate of the sample decreases initially and increases again as the area ratio decreases. At the copper pattern to board ratio of 10/100 and 100/100, the heating rates with and without the quartz substrate are similar. However, in the middle range of area ratios (i.e., area ratio = 23/100, 40/100, 63/100), the heating rates of the samples on the quartz substrate are significantly lower compared to those without the quartz substrate.

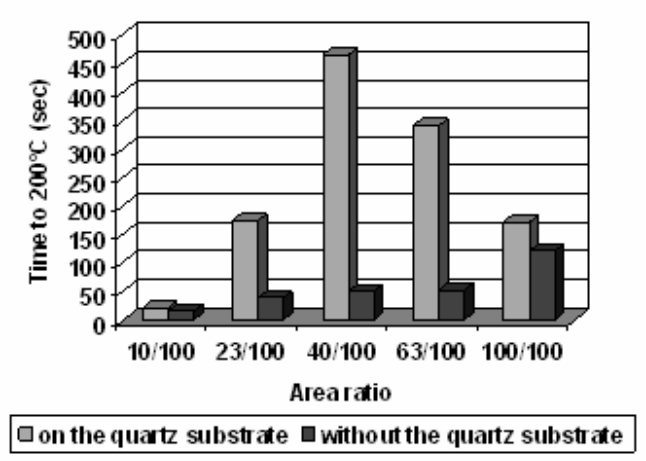

Fig. 8. The heating rates of square patterned BT boards with a full surface copper cladding on the bottom at a constant microwave power of 500W.

The overall goal of this study is to examine the feasibility of VFM curing of high performance dielectric materials on BT boards. Hence, the effect of the presence of a dielectric polymer on the heating rate of the board is studied. In Fig. 9, the heating rates of PI 2611 coated on a double Cu clad board, on a single Cu clad board and on a bare BT board were examined. In addition, these results were compared to the heating rates for boards without PI 2611. The bare BT board coated with PI 2611 shows a higher heating rate than the bare BT board without PI 2611. This indicates that the presence of a PI 2611 film, which initially has a high dielectric loss due to its uncured state, and the presence of NMP solvent, increases the absorbance of microwave energy. Initially, the PI 2611 coated BT board with a copper cladding on the top heats slightly faster than the same board without PI 2611. However, at temperatures above 180°C, the impact of PI 2611 on the heating rate is less because the contribution of the solvent diminishes as it evaporates and the polymer cures. The heating rate of the double copper clad BT board was not improved by the addition of PI 2611.

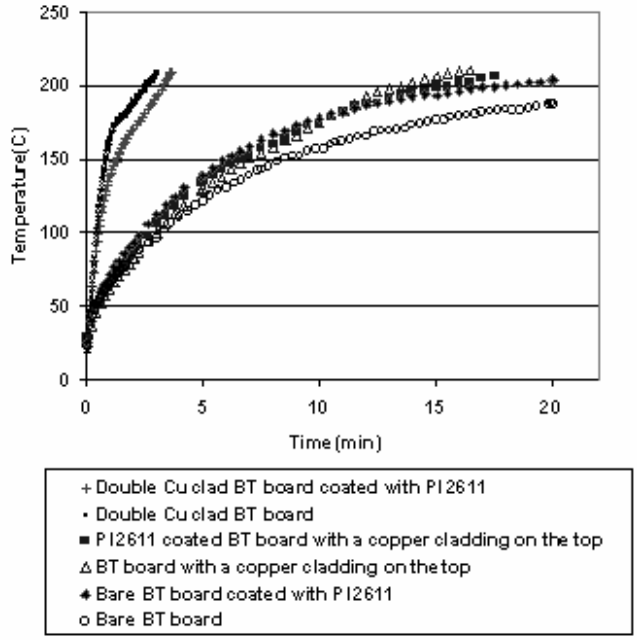

Fig. 9. The VFM heating curves of BT boards coated with the PI2611 films at the constant microwave power of 500W.

The degrees of curing of PI 2611 cured on the BT board with and without copper were compared as shown in Fig. 10. The microwave power of 500W was used to ramp the final temperature of 200ºC. The time to reach 200ºC was different for each of the three substrates. To compensate for these differences, each sample was held for an additional

30 minutes, once a surface temperature of 200ºC was obtained. The degree of curing of the polymer film decreases as the substrate changes from double copper clad BT board to single copper clad BT board to bare BT board. Thus, it must be assumed that there is a temperature gradient in the film. Although the surface temperature of the films are all at 200ºC, the interior temperature of the substrates is highest in the double copper clad BT board and lowest in the bare BT board.

Fig. 10 also shows the variation of degree of curing from the center to the edge. The variation of the degree of curing is significant on the bare BT board compared to other two BT board, because the bare BT board does not have a thermally conductive copper cladding that can distribute the heat to the edges efficiently. In microwave processing, the heat loss through the edge is expected since the surroundings of the samples are relatively cool.

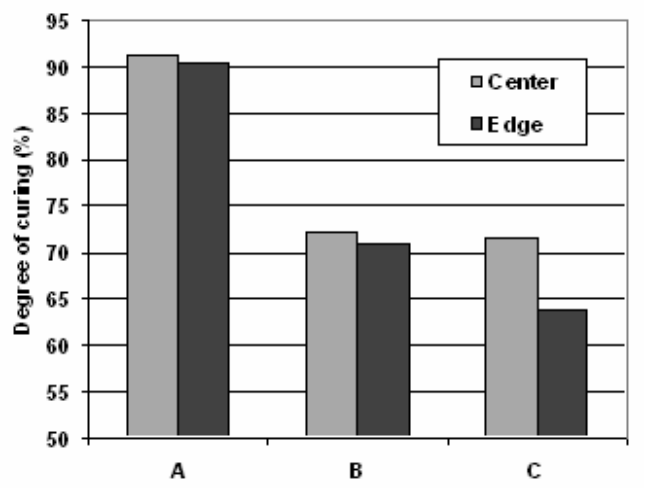

Fig. 10. The variation of the degree of curing according to the substrates at the VFM curing condition of 200°C for 30min. A: double copper clad BT board, B: BT board with a copper cladding on the top, C: bare BT board.

It is important not only to demonstrate that it is feasible to VFM cure polyimides on a BT substrate, but also show that the final film problems of VFM cure and thermally cured polyimides are similar. The properties of PI 2611 cured on the BT boards with and without copper cladding are shown in Table 1. The cure conditions were adjusted so that the BT substrate did not degrade more than the acceptable amount, equivalent to heating a board to 220ºC for one hour. The heating rate, 15ºC/min was used for the double copper clad BT board. The heating rate for single copper clad and bare BT board is the average heating rate achieved by the microwave power of 500 W. Table 1 shows that VFM cured PI 2611 has a similar degree of curing and the Young's modulus to thermally cured PI 2611. However, VFM cured PI 2611 shows a 17 ~ 28°C lower 1% weight loss temperature than thermally cured PI 2611. Since the degree of curing is the same, the lower 1% weight loss temperature of VFM cured PI 2611 is most probably due to the higher residual solvent content. The solvent NMP has a normal boiling point of 202ºC. Because of a lower 1% loss temperature with a similar degree of curing, VFM cured PI 2611 has a higher dielectric constant and the higher loss tangent than thermally cured PI 2611.

Table 1.
The properties of PI 2611 cured on BT boards using VFM cure conditions which yield a board degradation level of 220°C 1hr.

Properties	VFM			Thermal
	Double Cu clad	Single CU / top	Bare BT	
Curing condition	15˚C/min 200˚C, 15min	10.5˚C/min 220˚C, 15min	5.5˚C/min 240˚C, 0min	5˚C/min 200˚C, 1hr
Extent of Curing (%)	91	93	84.1	90.2
Young's modulus	7.9	8.2	-	8.2
1% weight loss temperature (˚C)	232	243	-	260
Dielectric constant	4.05	3.92	-	3.77
Loss tangent	0.0076	0.0055	-	0.0049

The properties of Cyclotene 3022 cured on the BT boards with and without metal cladding are shown in Table 2. Comparing the properties of VFM cured and thermally cured Cyclotene 3022, VFM cured Cyclotene 3022 shows a higher degree of curing than the thermally cured Cyclotene 3022. The 1% weight loss temperature of VFM cured Cyclotene is almost the same as that of thermally cured Cyclotene 3022. Since the curing temperature is much higher than the boiling point of mesitylene (165ºC), the presence of residual solvent appears not to be an issue in the VFM curing of Cyclotene 3022. Because of the higher degree of curing with a similar 1% weight loss temperature, VFM cured Cyclotene 3022 shows a lower dielectric constant and lower loss tangent than thermally cured Cyclotene 3022.

Table 2.
The properties of Cyclotene 3022 cured on the full surface copper clad BT board at VFM curing conditions which yield a board degradation level of 220°C 1hr.

Properties	VFM		Thermal
	Double Cu clad	Single CU / top	
Curing condition	15˚C/min 200˚C, 15min	5.4˚C/min 220˚C, 15min	5˚C/min 200˚C, 1hr
Extent of Curing (%)	87.2	86.8	80.3
1% weight loss temperature (˚C)	391	392	390
Dielectric constant	2.73	2.79	2.85
Loss tangent	0.0016	0.002	0.0023

To study the effect of the shape of the copper patterns on the curing of polymer films (in contrast to polymer cured on a full copper clad surface), various copper patterns (including squares, circles and broken copper lines) were prepared. PI 2611 polyimide was spin-coated on the samples. Each sample was heated next to a double copper clad BT board that served as a reference to measure the temperature. The temperature was measured in the middle of the reference double copper clad BT board. The temperature of the double copper clad BT board was increased at a constant ramp rate of 15°C/min.

BT boards with the square copper patterns on the top and a full surface copper layers on the bottom showed severe degradation in the square patterned region when the temperature of the double copper clad BT board was 215°C, as is indicated in Table 3. Generally, severe board degradation occurs at a temperature above 250°C. Thus, the temperature of the board near square patterned region is above 250°C when the temperature of the double copper clad BT board is 215°C. The heating rate of the square patterned BT board without a copper cladding on the bottom shows severe degradation when the reference double clad board is at a temperature of 185ºC, indicating that the square patterned BT board without copper cladding heats at a much faster than the square patterned BT board with a bottom copper cladding. As it can be seen from the comparison of the temperature of the reference double copper clad BT board in Table 3, the heating rate of BT board with 100 μm × 9 mm lines is the highest and the heating rate of a circle patterned BT board is the lowest.

Table3.

The relative heating rate of the BT board with the copper patterns (The area ratio of the square and circle pattern to the sample is 10/100).

Top of the BT Board	Bottom of the BT Board	Temperature of the double copper clad BT board	Degree of curing (%)	Region of the BT board
Square copper pattern	Full surface copper cladding	215˚C	Severe degradation in the square patterned region	
		200˚C	94.7	Square patterned region
			0	Outside region of the square pattern
	No copper cladding	185˚C	Severe degradation in the outside region of copper pattern	
		165˚C	0	The whole region except the corner of the square pattern
			39	Corner of square pattern
Circle copper pattern	No copper cladding	220˚C	Severe degradation in bare BT region	
		200˚C	38	Circle patterned region
			0	Outside region of the circle pattern
100 μm wide 9mm copper lines	Full surface copper cladding	140˚C	Severe degradation between the ends of lines	
	No copper cladding	100˚C	Severe degradation between the ends of lines	

The temperature is not uniform across the copper patterned BT board. In the squared patterned BT board with a copper cladding on the bottom, the degree of curing is close to 100% for the square copper patterned region, while there is virtually no curing in the outside region of the square patterned region when the temperature of the double copper clad BT board was 200°C. Further, severe degradation occurred only in the square patterned region when the temperature of the double copper clad BT board is 215°C. This indicates that the square patterned region is at a higher temperature than the outside region of the square pattern.

In the square patterned BT board without a copper cladding on the bottom, the curing is only significant in the regions at the corner of the square pattern when the temperature of the double copper clad BT board is 165°C. The severe degradation occurs only in the outside region of the square pattern when the temperature of the double copper clad is 185°C. This indicates that severe heating begins to takes place at the corners of the square pattern, and the board degradation propagates from the corners of the square pattern to the outside region of the square pattern.

The circle patterned BT board without a full surface copper cladding on the bottom shows the severe degradation when the temperature of the reference double copper clad is 220°C. This temperature is 35°C higher as compared to that of the square patterned BT board with bare BT on the bottom. Thus, the heating rate of the circle patterned BT board is slower than that of the square patterned BT board. It is also shown that at the temperature of the double copper

clad, 200°C, the circle patterned BT board without a full surface copper cladding on the bottom shows 38% degree of curing in the circle patterned region, but there is almost no cure in the outside region of the circle pattern.

BT boards with 100 μm wide by 9 mm long line segments across the board have the highest heating rate as it can be seen from the lowest temperature of the double clad where the severe degradation occurs. Severe degradation was observed in the region where the ends of the line segments (i.e corners of the lines) are concentrated. The full surface copper cladding on the bottom reduces the severe heating at the corner as it can be seen from the higher temperature of the double copper clad BT board, 140°C, of the BT board with the full surface copper cladding than 100°C of the BT board without the full surface copper cladding as shown in Table 3.

Table 4 shows the degrees of curing of PI 2611 and Cyclotene 3022 cured by VFM on BT boards with 100 μm × 9 mm line segments and the board degradation levels. The degradation levels reported in Table 4 are those in the region between the ends of the copper lines where the degradation is highest. For the VFM curing of PI 2611 on the BT board with no surface copper cladding on the bottom at 200°C for 5 min, the board degradation level is 220°C, 3hr ~ 240°C, 1hr. The board degradation level is reduced to 220°C 1hr ~ 220°C 3hr, when the Cyclotene 3022 is cured on the same BT board by VFM at 220°C for 15 min, even though the hold time was longer than in the polyimide cure.

Table 4
The extents of curing of PI 2611 cured on the BT boards with 100 μm short line patterns on the top and the board degradation levels.

Polymer	Cure Tech.	Bottom of the BT Board	Curing condition	Degree of curing (%)	Board degradation
PI 2611	VFM	No copper cladding	15°C/min, 200°C, 5 min	73.1	200°C, 3hr~ 240°C, 1hr
Cyclotene 3022	VFM	No copper cladding	15°C/min, 220°C, 15 min	74.8	220°C, 1hr~ 220°C, 3hr
	VFM	Full surface Cu cladding	15°C/min, 220°C, 30 min	87	220°C, 1hr
	Thermal	-	5°C/min, 220°C, 1hr	80	220°C, 1hr

Table 4 also shows the effect of the full surface copper cladding on the board degradation. The board degradation level is 220°C, 1hr ~ 220°C, 3hr for the VFM curing of Cyclotene 3022 on the BT board with no copper cladding on the bottom exposed to curing conditions involving a hold temperature of 220°C for 15 minutes. The board degradation level is reduced to 220°C, 1hr when Cyclotene 3022 is cured by VFM on the BT board with a full surface copper cladding on the bottom under cure conditions involving a hold temperature of 220°C for 30 minutes. The full surface copper cladding on the bottom reduces the board degradation. A higher degree of curing on the BT board with a full surface copper cladding on the bottom by VFM was achieved compared to thermally cured Cyclotene 3022 at the same board degradation level, 220°C, 1hr.

Aluminum foil was placed on the film surface of single copper clad BT boards coated with PI 2611 to increase the heating rate by the waveguide effect. The heating curves of PI 2611-coated BT boards with the aluminum foil are shown in Fig. 11. For the BT board with a copper cladding on the top, the PI 2611 film was between the aluminum foil and the copper cladding. For the BT board with a copper cladding on the bottom, the PI 2611 film and the BT board were sandwiched between the aluminum foil and the copper cladding. When aluminum foil was covering the PI 2611-coated BT board with a copper cladding on the top, the heating rate increases slightly. However, the heating rate of the PI 2611-coated BT board with a copper cladding on the bottom increases significantly with the aluminum foil on top.

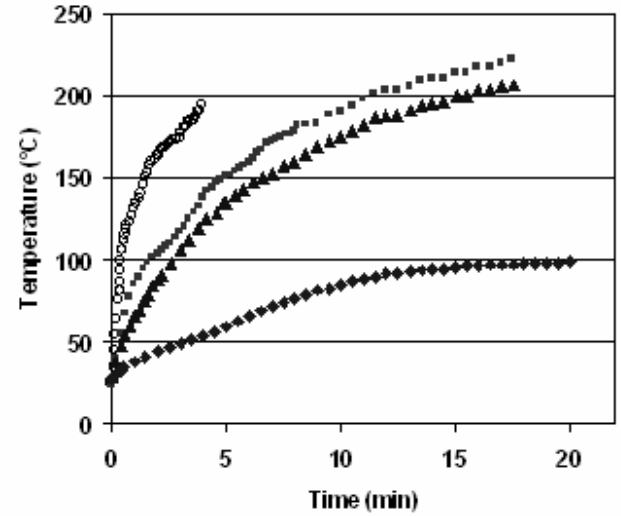

Fig. 11. The heating rates of PI 2611 coated BT boards covered with aluminum foils. ○: Al foil on the PI 2611 coated BT board with a copper cladding on the bottom, ■: Al foil on the PI 2611 coated BT board with a copper cladding on top, ▲: PI 2611 coated BT board with a copper cladding on the top, ♦: PI 2611 coated BT board with a copper cladding on the bottom.

5.0 Discussion

The VFM heating characteristics of full surface copper clad BT boards depend on the copper configuration and the quartz substrate. Without the quartz substrate, the double copper clad BT board shows a similar heating rate to the bare BT board (Fig. 3). This is due to the heating of the BT board between the double copper claddings, as the parallel metal plates guide the microwaves. The microwaves come from the edge opening and propagate between the double copper claddings. The BT board between the double copper claddings absorbs the microwave energy and heating of the entire sample results. Therefore, the heating rates of the double copper clad BT board and the bare BT board are similar. The parallel double copper claddings maintain the high rate of heating of the bare BT board. As shown in Fig. 5, the heating rate decreases significantly when the edge opening of the double copper clad boards is covered with the copper tape.

It is also shown in Fig. 3 that the heating rate of the BT board with a copper cladding on the top or bottom without the quartz substrate is significantly lower than the heating rates of the double copper clad BT board and the bare BT board. This is due to the interaction of the microwaves and the conductor surface. When the electromagnetic waves are incident upon the conductor surface, planes where the intensity of the electric field is zero are formed periodically due to the interference of the waves propagate toward and reflected from the conductor surface [14]. For the waves with a wavelength λ, and an incident angle upon the conductor surface of θ, the first maximum intensity of the electric field occurs at a distance, $\lambda/(4\cos\theta)$, from the conductor surface. The intensity of the electric field is zero at the conductor surface. The copper cladding of the BT board with a copper cladding on one side acts as a conductor surface. For the average wavelength of VFM of 4.7 cm and an incident angle of 45°, the maximum electric field intensity occur at 1.65 cm from the conductor surface. The thickness of the BT board attached to copper cladding is about 1 mm, and hence, the intensity of the electric field in the BT board will be very weak in comparison to the maximum intensity at 1.65 cm from the copper cladding. Due to the weak electric field, the heating rate of the BT board with a copper cladding on the top or bottom is significantly slower than the double copper clad BT board and the bare BT board.

The quartz substrate changes the heating rates of the full surface copper clad BT boards significantly, comparing the heating rates shown in Fig. 3 and Fig. 4. It appears that the quartz substrate partially reflects the microwaves and acts similarly as a copper cladding. The proposed effect of the quartz substrate is shown in Fig. 12. The heating rate of the bare BT board decreases when placed on the quartz substrate compared to that without the quartz substrate. This is similar to the observation that the heating rate of the bare BT board without the quartz substrate decreases significantly when one side of the board is covered with a copper cladding. The quartz substrate weakens the intensity of electric field in bare BT board as does the copper cladding of the BT board with a copper cladding on one side, and the heating rate of bare BT board is reduced on the quartz substrate (Fig. 12(a)).

The heating rate of the BT board with a copper cladding on the top increases on the quartz substrate compared to the heating rate without the quartz substrate. This is similar to the observation that the heating rate of the BT board with a copper cladding on the top without the quartz substrate increases when the remaining bottom side is also covered with a copper cladding (i.e., double copper clad BT board). The copper cladding on the top of the BT board and the quartz substrate at the bottom guide the microwaves as in the double copper clad BT board, and the heating of BT board between the copper cladding and the quartz substrate occurs (Fig. 12(b)).

However, the heating rates of the double copper clad BT board and the BT board with a copper cladding on the bottom do not change much on the quartz substrate. In the double copper clad BT board and the BT board with a copper cladding on the bottom, the microwaves reflect on the copper cladding, regardless of the presence of the quartz substrate (Fig. 12(c), (d)). As a result, there is no effect of the quartz substrate on the heating rate of double clad BT board and BT board with copper cladding on the bottom.

The VFM heating characteristics of the BT boards with copper patterns are different from those of the full surface copper clad BT boards. The degree of curing of PI 2611 was only high in the copper patterned region of the square patterned BT board with a full surface copper cladding on the bottom as shown in Table 3. The square patterned region is covered with copper on both sides. The outside region of the square pattern is covered with copper on the bottom. As discussed in Fig. 4, the heating rate of the BT board with copper on both sides is much faster than that of the BT board with copper the bottom. Therefore, the square patterned region is at a higher temperature compared with the outside region of the square pattern.

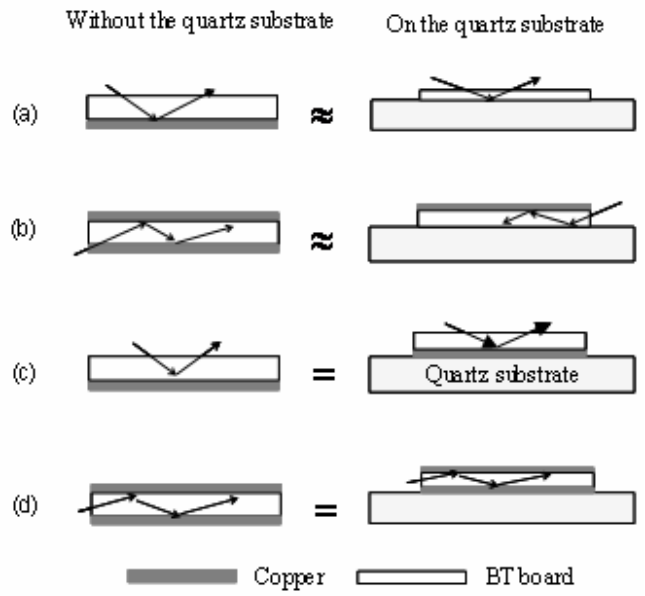

Fig. 12. The similarity in structure of BT board on quartz substrate with BT board without substrate

When there is no copper cladding on the bottom of the board, the square patterned region is covered with copper on the top and the outside region of the square pattern has no copper. Severe degradation occurred in the outside region of the square pattern as shown in Table 3. In addition, the higher degree of curing was observed only at the corners of the square patterns at a higher temperature. This is due to the electric field focusing at the corners of the square pattern. It is well known that the charges build up at edges or corners of conductors under a static electric field, and the electric field intensity is high at these regions [15]. In addition, the electric fields focus at the corners in microwave processing and severe heating can take place [16].

The electric field focusing is observed to be most significant in BT boards with 100 μm × 9 mm lines segments. The electric field focusing effect is severe in these regions where corners are concentrated (i.e. between the ends of the line segments), and hence, the degradation is highest in these regions. The BT board with 100 μm straight lines showed a slower heating rate than the BT board with 100 μm × 9 mm lines, because 100 μm wide straight lines does not have discontinuities in the lines that can induce the electric field focusing.

The electric field focusing is reduced when the full surface copper cladding is on the bottom of the BT board. Comparing the square or 100 μm × 9 mm line segment patterned BT boards, the electric field focusing at the corners is not severe when there is a full surface copper cladding on the bottom as shown in Table 3 and Fig. 6. Also, it is shown in Table 4 that the board degradation is lower in the 100 μm × 9 mm lines patterned BT board with a full surface copper cladding, even with a longer hold time at a same curing temperature, compared to the 100 μm × 9 mm lines patterned BT board without a full surface copper cladding. Without the full surface copper cladding, the electric fields focus in the horizontal direction as shown in Fig. 13(a). The electric field focusing is reduced by distributing the electric field vectors in the vertical direction when there is a full surface copper cladding on the bottom as shown in Fig. 13(b). The intensity of the electric field is weak in the region with copper on one side and the electric field intensity will be weak at the corners above the full surface copper cladding.

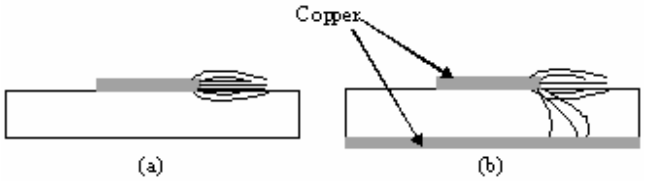

Fig. 13. The schematic diagram of the electric field focusing at the corner of the square pattern. (a) Without a copper cladding on the bottom. (b) With a copper cladding on the bottom.

Fig. 8 shows the heating rates of the square patterned BT boards with a copper cladding on the bottom. Without the quartz substrate, the heating rate decreases as the copper area ratio decreases. This is because the contribution of the heat generated at the corner of the square pattern by the electric field focusing becomes dominant, as the area of the pattern decreases. As the copper area ratio decreases from 100/100 to 63/100, the heating rate on the quartz substrate decreases. The temperature of the outside region of square pattern is significantly lower than that of the square patterned region. Thus, the heat generated in the square patterned region is transferred to the quartz substrate through the outside region of square pattern. This cooling effect increases as the area ratio decreases from 100/100 to 63/100. However, the heating rate on the quartz substrate increases again as the copper area ratio decreases further from 40/100 to 10/100. The efficiency of the heat removal through the outside region of square pattern decreases as the heat generation in the square patterned region becomes significantly rapid.

VFM accelerates the curing reaction of PI 2611. Table 1 shows that VFM curing gives a similar degree of curing for PI 2611 with a shorter time, compared to conventional thermal curing. However, the solvent evaporation is not accelerated by VFM curing of PI 2611. VFM cured PI 2611

shows a lower 1% weight loss temperature compared thermally cured PI 2611 as shown in Table 1. The solvent evaporation is less of an issue in VFM curing of Cyclotene 3022. As shown in Table 2, the 1% loss temperature of VFM cured Cyclotene 3022 is similar to that of thermally cured Cyclotene 3022. 1% weight loss temperature of VFM cured Cyclotene 3022 shown is almost the same as that of fully cured Cyclotene 3022 according to thermal standard condition. This is because the boiling point of mesitylene, 165°C, is much lower than the VFM curing temperature, 200°C ~ 220°C.

The curing reaction is less accelerated in PI 2611 by VFM compared to Cyclotene 3022. VFM cured Cyclotene 3022 shows a higher degree of curing than thermally cured Cyclotene 3022 as shown in Table 2. The degree of curing of VFM cured PI 2611 is similar compared to that of thermally cured film as discussed before. This can be explained by the solvent effect in PI 2611. In the polyimides, the complexation between the NMP and the carboxylic acid or amide group in polyamic acid is observed [17, 18]. The different stages of the cure reaction require the decomplexation of the solvent from these groups for the cyclic ring-closing reaction to occur [18]. Hence, the curing reaction seems to be less accelerated by VFM in PI 2611 due to the high residual solvent content. A higher solvent content would also result in a higher dielectric constant and a higher 1% weight loss temperature shown in Table 1.

The board degradation is less severe in the VFM curing of Cyclotene 3022 on BT board with 100μm copper lines compared to PI 2611. The board degradation level of the BT board with 100 μm × 9 mm lines is lower in Cyclotene 3022, even though the curing condition is 20°C higher with 10min longer time than that of PI 2611 as shown in Table 4. In microwave processing, the charges will accumulate at the ends of the copper lines. Because of the charge build-up, an intense electric field is formed between the ends of the copper lines as discussed previously. The higher dielectric constant of the over-coating material enhances the charge build-up in the ends of the copper lines. Also, the higher dielectric constant and the higher loss tangent of the over-coating material induce higher microwave heating according to (1). Therefore, more severe degradation would occur between the ends of the copper lines for the over-coating material with the high dielectric constant and the high loss tangent. As it can be seen from the Tables 1 and 2, the dielectric constant and the loss tangent of Cyclotene 3022 are much lower at the same curing condition compared to those of PI 2611. Therefore, the board degradation is lower in VFM curing of Cyclotene 3022 on BT board with 100 μm × 9 mm lines.

With the aluminum foil on top of the PI 2611 film surface, the heating rate of the PI 2611-coated BT board with a copper cladding on the bottom increases significantly as shown in Fig. 11. The BT board between the aluminum foil and the copper cladding heats rapidly by the waveguide effect. This is a result of the bare BT board itself has a high heating rate as shown in Fig. 3, and the suppressed heating by the single copper cladding is increased by the waveguide effect. However, the heating rate of the PI 2611-coated 'Single Cu/ top' increased slightly when the aluminum foil was covered on top. This is due to the slow heating rate of the PI 2611 film itself, and the increased heating of the PI 2611 is not achieved by the waveguide effect of the aluminum foil and the copper cladding. PI 2611 has much a lower dielectric constant and a lower loss tangent than BT board, and the microwave heating of PI 2611 is much inefficient than the bare BT board.

6.0 Conclusions

The VFM heating characteristics of metallized BT boards was investigated. The VFM heating rate of the full surface copper clad BT board depended on the copper cladding configurations, and the presence of the quartz substrate under the BT boards. Electric field focusing was observed in BT boards with small copper patterns, and the board degradation was higher in the electric field focused regions. The full surface copper cladding on the bottom of the BT board reduced the field focusing. It was found that the electric field focusing disappears with fine circle copper patterns. The VFM curing of low-k polymers on the metallized BT boards was also studied. The heating rate difference of the polymer film and the substrate was important factor determining the curing condition on full surface copper clad BT boards. For VFM curing of low-k polymers on the BT boards with 100 μm × 9 mm lines segments, the dielectric constant and the loss tangent of the polymer were key factors determining the board degradation levels. Residual solvent left retained in the polymer after VFM curing can impact electrical, mechanical and thermal properties. Hence, polymers containing lower boiling point solvents have greater potential for use of VFM curing on metallized organic boards.

References

[1] International Technology Roadmap for Semiconductors, Assembly and Packaging, 2001 Edition.

[2] Tadanori Shimoto, Koji Matsui, Katsumi Kikuchi, Yuzo Shimada, and Kauzki Utsumi, "New high-density multilayer technology on PCB", IEEE transactions on Advanced Packaging, Vol. 22, No. 2, pp. 116-122, 1999.

[3] Raj, P. M., Shinotani, K., Seo, M., Zweben, C., Shiva Kumar, K., Bhattacharya, S., White, G. E., and Tummala, R. R., "Selection and evaluation of materials for future System-On-Package Substrate", 51st Electronic Components and Technology Conference, pp. 1193-1200, 2001.

[4] Product selector guide, "Polyimides for microelectronics", HD Microsystems.

[5] Cyclotene technical note, "Processing procedures for dry etch Cyclotene advanced electronic resins (dry etch BCB", The Dow Chemical Company.

[6] G 200 Product bulletin, Isola Laminate Systems.

[7] B. Panchapakesan, Patricia F. Mead, Zak Fathi, and Denise Tucker, "Variable frequency microwave: A new approach to curing", Advanced Packaging, Vol. 60, 1997.

[8] Kim Farnsworth, Manepalli R.H., Bidstrup-Allen S. A., and Paul A. Kohl, "Variable frequency microwave curing of 3,3'-4,4-biphenyltetracarboxylic acid dianhydride/p-phenylenediamine (BPDA/PPD)", International Journal of Microcircuits and Electronic Pakaging, Vol. 23, No. 2, pp. 162-171, 2000.

[9] Kim Farnsworth, Manepalli R. H., Bidstrup-Allen S. A., and Paul A. Kohl, "Variable frequency microwave curing of photosensitive polyimides", IEEE Transactions on Components and Packaging Technology, Vol. 24, No. 3, pp. 474-481, 2001.

[10] Ravindra V. Tanikella, Sue A. Bidstrup Allen, Paul A. Kohl, "Variable-frequency microwave curing of benzocyclobutene", Journal of Applied Polymer Science, Vol. 83, pp. 3055-3067, 2002.

[11] Ravindra V. Tanikella, "Variable Frequency Microwave Processing of Materials for Microelectronics applications, Ph. D. dissertation, Georgia Institute of Technology, 2003.

[12] National Materials Advisory Board, "Microwave processing of materials", Natioanl Academy Press, Washington, D. C., 1994.

[13] Taehyun Sung, "Variable Frequency Microwave Curing of Polymer Dielectrics on Metallized Organic Substrate, M. S. dissertation, Georgia Institute of Technology, 2003.

[14] David K. Cheng, "Field and wave electromagnetics", Addison-Wesley Publish, 1992.

[15] Halliday Resnick, "Fundamentals of physics", Johns Wiley & Sons, 1988.

[16] Roger Meredith, "Engineer's handbook of industrial microwave heating", IEE Power Series, The Institute of Electrical Engineers, London, 1998.

[17] Tzu-Chien J. Hsu and Zu-Ling Liu, "Solvent effect on the curing of polyimide resins, Journal of Applied Polymer Science", Vol. 46, pp. 1821-1333, 1992.

[18] M. -J. Brekner and C. Feger, "Curing studies of a polyimide precursor", Journal of Polymer Science: Part A: Polymer Chemistry, Vol. 25, pp. 2005-2020, 1987.